ARTICLE

Check for updates

Shell thickness of *Nucella lapillus* in the North Sea increased over the last 130 years despite ocean acidification

Dennis Mayk [1,2✉], Lloyd S. Peck [1], Thierry Backeljau[3,4] & Elizabeth M. Harper[1,2]

Ocean acidification and global climate change are predicted to negatively impact marine calcifiers, with species inhabiting the intertidal zone being especially vulnerable. Current predictions of organism responses to projected changes are largely based on relatively short to medium term experiments over periods of a few days to a few years. Here we look at responses over a longer time span and present a 130-year shell shape and shell thickness record from archival museum collections of the marine intertidal predatory gastropod *Nucella lapillus*. We used multivariate ecological models to identify significant morphological trends through time and along environmental gradients and show that, contrary to global predictions, local *N. lapillus* populations built continuously thicker shells while maintaining a consistent shell shape throughout the last century.

[1] Department of Earth Sciences, University of Cambridge, Downing Street, Cambridge CB2 3EQ, UK. [2] British Antarctic Survey, High Cross, Madingley Road, Cambridge CB3 0ET, UK. [3] Royal Belgian Institute of Natural Sciences, Brussels, Belgium. [4] Evolutionary Ecology Group, University of Antwerp, Antwerp, Belgium. ✉email: dm807@cam.ac.uk

With the increase of carbon dioxide in the atmosphere accompanied by a rise in (seawater) temperature, ocean acidification (OA; decreasing seawater pH and accompanying decrease in carbonate ion concentration), and more frequent extreme weather events, many marine species and ecosystems are at risk. In recent years, much effort has been made to study the impact of ocean warming, OA and the synergistic mixed effects of both on the development and survival of species at risk[1–7]. Special attention was given to studying the impacts on larval development[8–12] and biomineralisation in both juveniles and adults, especially in calcium carbonate ($CaCO_3$) shell-bearing species[13–16] as those are believed to be most impacted by global climate change[2,17,18]. Despite these efforts, our understanding of, and ability to predict future changes in global or regional ecosystems, assemblages, populations, or even single species are still limited.

Many relatively short-term experiments ranging from days to a few years report predominantly negative impacts on shell strength, size, and thickness of shell-forming marine species[13,19–21]. Yet, sometimes no such effects are observed or even reversed effects (e.g., shell thickening) are reported[15,22–24]. Long-term experiments accounting for phenotypic plasticity (within and across generations) and genetic adaptations are receiving increasingly more attention[25–28] as these processes are critical to allow for full phenotypic responses to the altered environment of the future ocean[29–31]. Conventional laboratory experiments often lack the variability and complexity of natural ecosystems by keeping relevant parameters stable to reduce the experimental "noise"[32]. This has the potential benefit of unmasking subtle responses that would otherwise remain unnoticed in inherently noisy biological systems[32]. However, these responses may not be representative of organisms in their natural environment, as spatial and temporal variability of temperature and of the carbonate system often already exceed the mean of anticipated future scenario changes. In addition, mixing of these factors and their variation could lead to unexpected organism responses[6]. This raises the important question of what influence environmental variability through time and space has at the species, community or ecosystem level[32]. Early efforts to answer this question suggested a significant effect of natural variability on individual species and changes to ecosystems, emphasising the non-linear relationship between environmental stressors and biological responses[6,33,34]. There are many examples of different responses between populations of a species between regions, for example, in relation to differing up-welling environments[35] or along latitudinal and salinity gradients[36]. Accordingly, more recent in situ studies have begun to highlight the complexities of the multitude of possible interactions between biological and other environmental factors in the mean phenotypic response and organism variability to a changing climate system[25,37]. Another approach to account for the inherent complexity of marine ecosystems is the use of archival museum collections to study phenotypic responses to historical changes in a particular species or population[22,31,38]. This approach offers a unique way to study organism responses, as it observes outcomes that, by their nature, include all natural organism–organism and organism–environment interactions at every given time interval. This allows the identification of organism or population responses in complex natural systems over considerably longer time frames, enabling us to extend the understanding gained from laboratory or in situ experiments. With overwhelming evidence pointing towards a change in community structures, habitats and ecosystems around the world, few study areas have remained natural which means that biological responses to modern environmental change are superimposed on already existing trends[39]. This makes it very difficult to identify organism responses to anthropogenically induced environmental change. Yet, in such cases palaeobiological data and archival assemblages, integrated with experimental data, can provide unique insights. For example, one

study found that modern *Mytilus californianus* in the northeastern Pacific build thinner shells than those archived from an American midden (1000–1340 AD)[40]. Other studies uncovered a substantial increase in shell calcite proportion over a 60-year period in *M. californianus* from the northeastern Pacific[22], and a substantial increase in shell thickness in archival *M. edulis* collections from the Southern North Sea across the 20th century[31].

The intertidal zone is a harsh and demanding environment in which sessile or slow-moving inhabitants are regularly exposed to a range of biotic and abiotic stressors, including varying water levels, wave action, air exposure, steep salinity gradients, large temperature variation and changing predator regimes. In terms of global climate change, the intertidal zone is considered one of the most vulnerable habitats as the interaction between global temperature rise and tidal movement may create a mosaic-like thermal environment that can be detrimental to intertidal organisms through, e.g., cardiac arrest or protein damage[41–43]. In addition, global climate change is expected to cause more extreme weather conditions[44–47], which will be accompanied by more frequent and more intense storm events, putting intertidal organisms at additional risk[48]. Intertidal organisms are adapted to hostile conditions, but an increase in the occurrence or duration of spatial and temporal stressor extremes as a consequence of global climate change may exceed their tolerance limits[49]. In addition to the natural stressors, anthropogenic interactions with the environment, e.g., through ship traffic, communal waste discharge, mining, tourism and agricultural land use, further exacerbate the hostility of the intertidal zone[50,51]. For example, increased land use for agricultural purposes and associated use of fertilisers resulted in a substantial nutrient burden from riverine input into the North Sea[52]. This resulted in eutrophication of the nearshore accompanied by an increase in primary production[52–54].

The carnivorous gastropod *Nucella lapillus* (Linnaeus, 1758) (dog whelk) is an important predator of the rocky intertidal shore in the Northern Atlantic[55,56] that exerts a strong top-down control on temperate rocky-shore ecosystems[57]. Due to its pronounced shell variability along environmental gradients such as wave energy and predator abundance[58–60], it has been the focus of numerous studies. Its calcareous shell consists of two distinct layers; irregular calcite externally and crossed lamellar aragonite internally, which may be separated by a transitional spherulitic layer[61]. The shell exhibits a high degree of variability in morphology[62–64], apertural teeth expression[65,66], and most notably, apertural thickness[58,59,65,67–69] in relation to environmental stressors. These characteristics make *N. lapillus* a valuable model for studying the impact of long-term environmental change on intertidal calcifiers. *Nucella lapillus* mostly preys on barnacles and mussels, which are important foundation species, shaping the morphology and habitat structure of the nearshore, providing shelter and facilitating the development of algal canopies and recruitment of other fauna[70]. These processes are key mechanisms to maintain and stabilise biodiversity and thus *N. lapillus* contributes considerably to the ecological stability of rocky shore communities and ecosystems. As a marine calcifier, it is likely that *N. lapillus* is vulnerable to the physico-chemical effects of global environmental change and investigating how this species is affected could be key to understanding and predicting how rocky-shore communities or ecosystems will change under future OA and ocean warming scenarios. To do so, we analysed key morphological parameters (shell layer thickness and shell shape) in the shell of archival *N. lapillus* samples collected between 1888 and 2019 from the Dutch and Belgian coasts in the Southern North Sea. This allowed us to identify important long-term in situ phenotypic responses to environmental change over the last 130 years. Shell thickness is a key metric used to study the

effect and vulnerability of species to OA, and shell shape variability provides an important direct measure of organism responses to new or changing environmental stressors[71]. Since both shape and thickness metrics are direct indicators of organism responses to environmental stress, they provide first-hand evidence of habitat degradation and thus allow to draw conclusions about habitat development over the studied period. To complement our observations, we analysed the observed phenotypic change in relation to long-term environmental change in wind speed (as a proxy for wave energy), air temperature, sea surface temperature, and salinity on the Southern North Sea coast using multivariate ecological models.

Results

Long-term trends in shell formation. We measured shell height, aperture size, shell outline shapes, and shell layer thickness from archival *N. lapillus* specimens and investigated respective trends through time using generalised additive mixed models (GAMMs). Shell height was used to provide a rough age estimation and allometric scaling in the GAMMs. Aperture size was used as a qualitative proxy to infer variations in wave energy regimes[72–74] and predation pressure[74]. Shell outline shapes (hereafter shape-PCs) as expressed by elliptic Fourier analysis and subsequent principal component analysis (PCA) (see the "Methods" section), were used to investigate phenotypic responses to environmental stressors[71,74], and shell layer thickness measurements (Fig. 1), were used to investigate the impact of a changing carbonate system on shell formation[18,23,24,40,75].

Shell outline analyses revealed pronounced shape variations between specimens, and we selected the first five shape-PCs as shell shape representatives that described different forms of shape variance between specimens (Fig. 2). The most pronounced shell shape variability accounting for 43% of the total shape variance among individuals, captured by shape-PC1, described a rounding of the shell. Shape-PC2 captured 18.3% of the shape variance among specimens describing a minor shift in the siphonal canal, and shape-PC3 described an inclination of the longitudinal axis encompassing 12.2% of the total shape variance. Shape-PC4 and shape-PC5 described minor shape variations capturing 6.1% and 4.8% of the total shape variance, respectively. Combined, these five principal components (shape-PC1–shape-PC5) captured 84.4% of the total shape variance among specimens and therefore provided a solid representation of the shape variance encompassed in the sampled specimens.

Shell shape models for aperture size and shape-PCs revealed a significant aperture size increase in *N. lapillus* specimens from 1888 until 2019 ($F_{1.75} = 5.24$, $p = 0.016$) by 14.2 mm^2, i.e., by 10% whereas shell shape-PCs remained remarkably stable throughout the last 130 years. Only shape-PC2 exhibited a weak but significant change trend (shape-PC2: $F_1 = 3.95$, $p = 0.047$) (Fig. 2, Supplementary Table 4). Although the model performed significantly better than an intercept-only model (null model), the deviance explained by the shape-PCs model was relatively low ($R^2_{adjusted}$: 0.11), suggesting that other unaccounted factors had a strong influence on the shell shape of the studied *N. lapillus* specimens.

In contrast to the shell shape stability, but in line with the increase in aperture size, shell layer thickness models for the aragonite and calcite layer both showed a significant increase in shell layer thickness from 1888 to 2019. Aragonite layer thickness significantly increased by 0.1 mm ($F_1 = 6.08$, $p = 0.015$), i.e., by 79%, calcite layer thickness increased significantly by 0.22 mm ($F_1 = 4.18$, $p = 0.043$), i.e., by 39%, and both shell layer thickness models performed significantly better than the respective intercept-only models. The GAMMs summary statistics of shell shape and thickness models are provided in Supplementary Table 4.

Environmental change. To investigate changes in environmental (global change driven) stressors along the Belgian and Dutch coast over the last 130 years, three key environmental parameters (wind speed, air temperature, and sea surface temperature) that provided sufficient long-term trends were selected, and their trends modelled using GAMMs (Fig. 3). In addition, we investigated the spatial variability in sea surface salinity between sampling sites (Supplementary Fig. 2b). We assessed salinity variation spatially instead of through time because nearshore salinity regimes generally exhibit a mosaic pattern due to surface and underground freshwater run-off, likely resulting in higher levels of variation across spatial scales than expected from decadal temporal data[31]. We also estimated yearly calcification windows (i.e., days per year when mean temperatures reached hypothetical threshold values allowing for optimal shell calcification/growth) from monthly mean temperatures and their standard deviations for the thresholds of 10–15 °C in 1 °C increments (Fig. 4). This was done because the somatic and shell growth of marine molluscs is, under normal circumstances, tightly linked to temperature[76,77] so that each species has a particular thermal optimum that is ideal for growth[78–81]. Although there are exceptions to this observation[82,83], biomineralisation rates can be greatly reduced or even halted when the environmental temperature falls below an organism or population-specific temperature threshold[76,79,84] making temperature thresholds an important environmental metric in the investigation of shell formation trends, especially over long temporal or spatial scales.

Unfortunately, we were unable to directly assess changes in seawater pH due to a lack of suitable long-term data. The reliable tracing of long-term trends in the seawater carbonate system requires data sets of at least 25 years[85] which are not available for the (Southern) North Sea[86]. However, as we explain in the discussion, the discharge of anthropogenic effluent over many decades had a considerable influence on the carbonate system of the Dutch and Belgian nearshore making the assessment of pH changes less relevant for the formation of biogenic CaCO$_3$ in this region[87].

The long-term models of the selected environmental parameters revealed an increase in air temperature, sea surface temperature and wind speed from 1880 to 2020 (Fig. 3, Supplementary Table 2). Mean air temperature increased significantly ($F_1 = 17.41$, $p < 0.001$) by 1 °C. Mean sea surface temperature increased significantly ($F_{4.59} = 25.78$, $p < 0.001$) by 2 °C with an acceleration of warming since 1985 to the present. The winter months from December to February exhibited the most pronounced increase in temperature of all months throughout the time series (Supplementary Fig. 3). The mean wind speed trend showed an initial drop from 1880 to 1930 by about 2 m s^{-1} after which it rose significantly ($F_{8.27} = 40.9$, $p < 0.001$) by 3 m s^{-1} to peak values in 1985. The GAMMs summary statistics of environmental trend models are provided in Supplementary Table 2.

Although the sampling sites were deliberately chosen to be in close proximity to each other (maximum distance ~49 km), spatial comparisons of salinity data confirmed the anticipated heterogeneity between sites (Kruskal–Wallis: $H(6) = 832.414$, $p < 0.001$). A pairwise Wilcoxon Rank Sum test with standard Bonferroni adjusted p-values for pairwise comparison of median salinities between each sampling site (Supplementary Table 3) revealed that the median salinity of 30.1 PSU at Zwarte Polder was significantly lower than those at the other sites. Median salinities at Blankenberge (30.9 PSU), Zeebrugge (30.9 PSU),
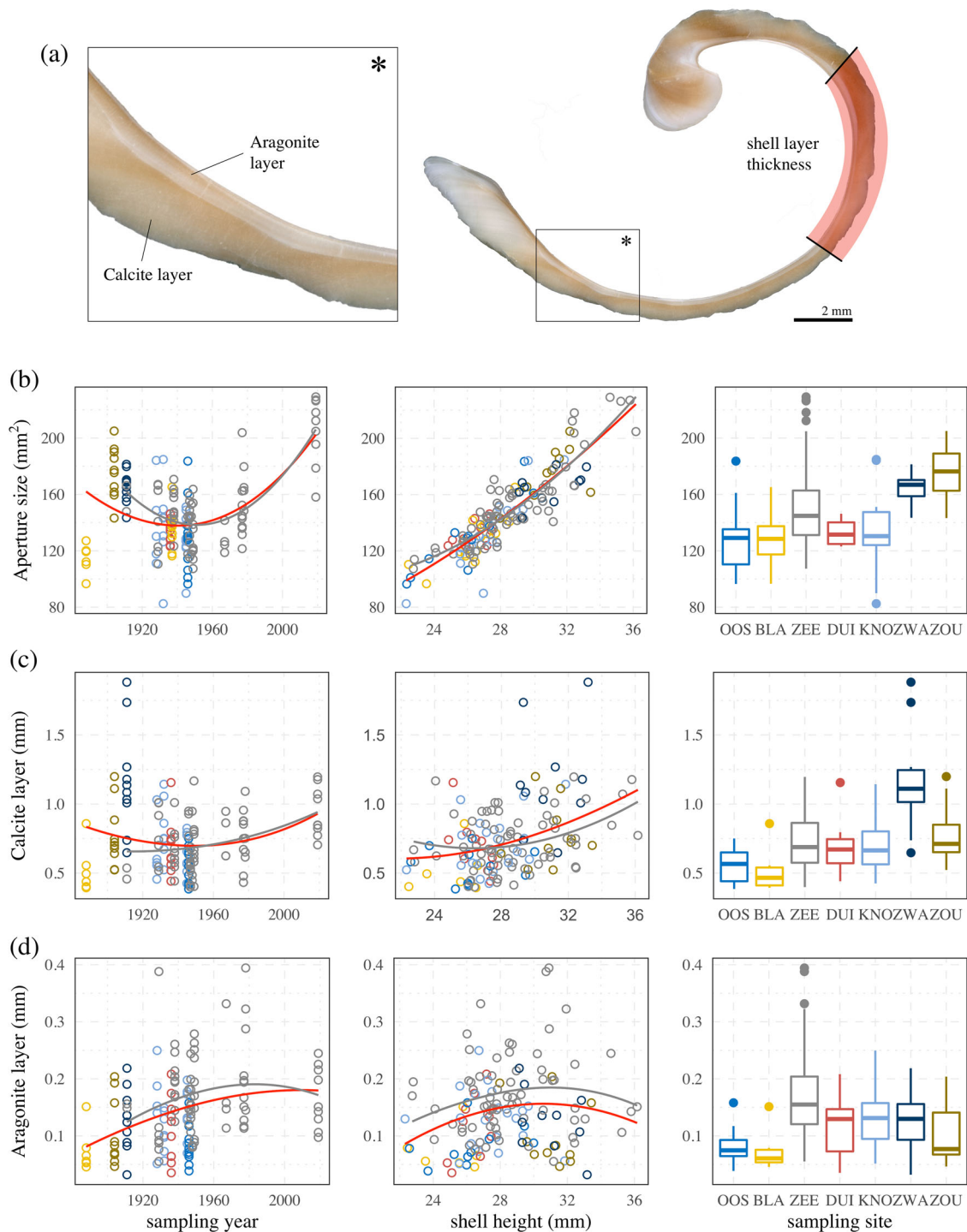
Fig. 1 Shell thickness and aperture size trends over the last century. a Image showing the section of shell used for the thickness analyses. The dorsal region where thickness measurements were carried out is highlighted in red. **b** Relationship of aperture size with sampling year, shell height and sampling sites. **c** Relationship of calcite layer thickness with sampling year, shell height and sampling sites. **d** Relationship of aragonite layer thickness with sampling year, shell height and sampling sites. Loess smoothing curves indicate trends for the whole dataset (red) and for samples collected at Zeebrugge only (blue). Sampling site abbreviations from west to east: OOS Oostende, BLA Blankenberge, ZEE Zeebrugge, DUI Duinbergen, KNO Knokke, ZWA Zwarte Polder, ZOU Zoutelande. Boxplot whiskers refer to the 1.5 interquartile range.

Duinbergen (30.8 PSU), and Knokke (30.9 PSU) were not significantly different, likely due to the proximity of these sites. Oostende exhibited a median salinity of 32.7 PSU, which is significantly higher than at all other sites. However, although statistically significant, variations in sea surface salinities between sampling sites appeared minor considering reported salinity differences of up to three times normal seawater salinity experienced by intertidal organisms in tidal pools[88].

Calcification window thresholds (10–15 °C) significantly increased non-linearly from 1880 until 2019 (Fig. 4). The percentage increases of days per year above temperature thresholds ranged from 27% to 123% depending on the threshold used.
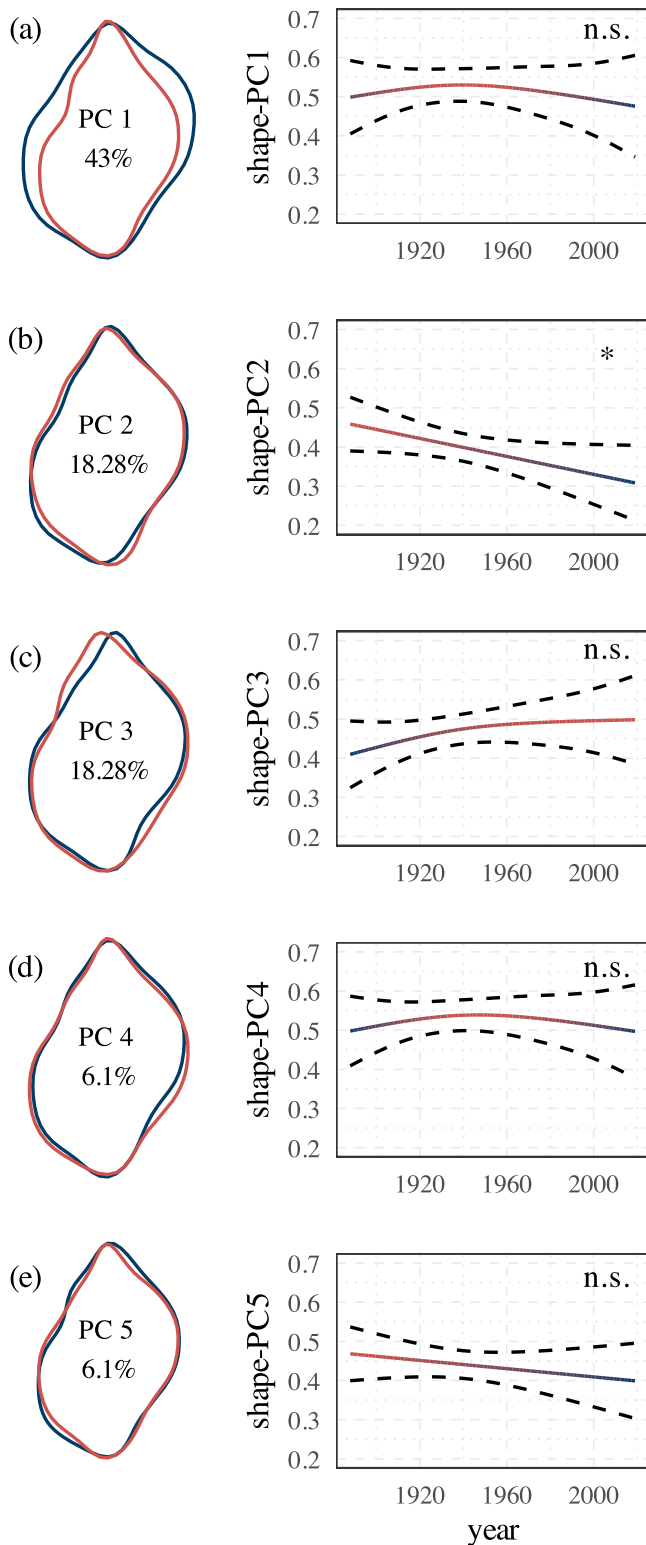
Fig. 2 Shell shape trends presented for the first five shape descriptors. **a** Shape-PC1, **b** shape-PC2, **c** shape-PC3, **d** shape-PC4, and **e** shape-PC5 in the intertidal gastropod *Nucella lapillus* from the Belgian and Dutch coast collected between 1888 and 2019. Shape variance ($\bar{x} \pm 3\sigma$) encompassed in either shape-PC is presented as outline extremes.

The biggest percentage increase was in the 15 °C temperature threshold group showing that there were more than twice as many days reaching sea surface temperatures of 15 °C in 2019 than in 1880.

Environmental impact on shell calcification. Relationships between environmental change and shell shape and shell thickness trends were investigated using GAMMs employing an automated model term selection process. To reduce dimensionality and thereby overcome potential complications with multicollinearity among environmental predictors, we constructed environmental regimes (PC1 and PC2) as expressed by PCA for each environmental descriptor (Fig. 5). The models revealed a significant relationship of aperture size with sea surface temperature and wind energy regimes and showed a strong but expected allometric relationship (Fig. 6). They also revealed a significant relationship between aragonite layer thickness and sea surface temperature and a significant correlation between calcite layer thickness and wind speed regimes. Both aragonite layer and calcite layer thickness showed significant relationships with the sampling site. The models further suggested a significant allometric relationship of shell shape and a significant relationship between shape-PC1 (describing the rounding of the shell) and sea surface temperature regimes. The GAMMs summary statistics for the constructed models are provided in Supplementary Table 5.

Discussion

Despite considerable environmental change (Fig. 3), our results suggest only minor long-term shell shape trends in *N. lapillus* on the Southern North Sea coast. Overall, shell shape varied more with the size of the animal than through time or along environmental gradients. Contrary to expected species responses to global climate change[21], we found significant increases in shell layer deposition in *N. lapillus* over the last 130 years (Fig. 7). In relative terms, aragonite layer thickness increased twice as much as calcite layer thickness, although in absolute terms calcite layer thickness increased more. However, unlike reported apertural lip thickening observed in archival *N. lapillus* from the US east coast that scaled solely with shell height[89], our shell thickness descriptors showed only weak allometric relationships and correlated significantly with collection year (Figs. 1 and 7).

Constraints on biomineralisation. Shell formation through $CaCO_3$ precipitation is most influenced by three factors: temperature[18,90], ion availability ($[Ca^{2+}]$ and $[HCO_3^-]$)[91] and the nutritional state of the organism, as shell formation comes with a cost in metabolic energy[92–94]. Since the solubility product of $CaCO_3$ in seawater is temperature dependent, changes in ambient temperature can have a sizeable influence on $CaCO_3$ saturation states. Low temperatures decrease the saturation state and, consequently, the precipitation rate of $CaCO_3$[95]. Low temperatures can also impair important cellular processes, so that higher temperatures generally facilitate shell formation. In addition, a limited availability of substrate abundance, i.e., $[Ca^{2+}]$ and/or (hydrogen-) bicarbonate ions, which are the building blocks of $CaCO_3$, may also impair shell production rates. For example, low $[Ca^{2+}]$ limit shell formation rates in mytilid mussels in the Baltic Sea[91]. Responses to these limitations, by, e.g., high latitude calcifiers, entails the incorporation of a larger proportion of organic material into their shell which in turn comes with an increase in metabolic cost per unit shell[36,93,94,96]. Estimates of the amount of energy required to produce a unit of shell vary largely between studies but may be as large as ~60% of the available assimilated energy, e.g., in blue mussels from the Baltic Sea and thus can contribute considerably to an organism's energy balance[96].

Stress due to increased wave action or increasing predator abundance may also affect shell formation rates. *Nucella lapillus* responds to increased predator abundance by growing thicker apertural lips with larger apertural teeth[65,74]. A study on shell layer thickening in archival blue mussels collected from adjacent locations to our sampling sites on the Belgian coast observed that
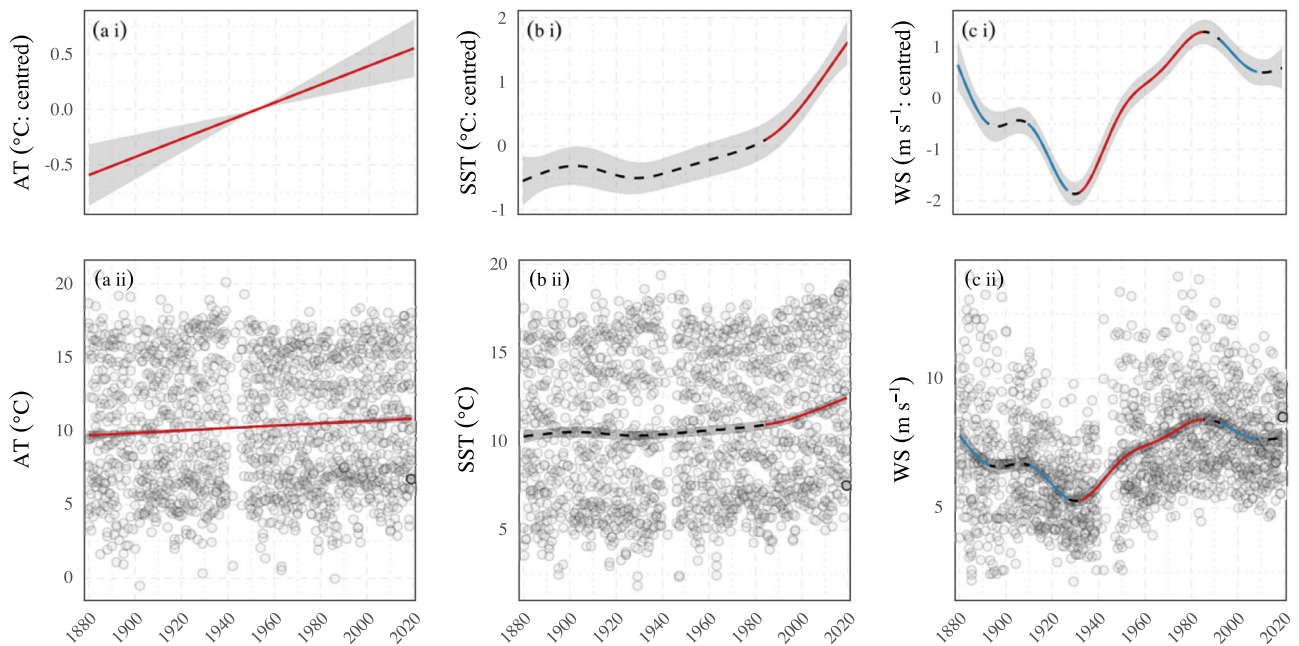
Fig. 3 Historical trends in temperature and wind speed on the Southern North Sea coast. Historical trends of **a** air temperature, **b** sea surface temperature, and **c** wind speed within the sampling region from 1880 to 2020. For each environmental parameter both the overall change including all individual data points (**a** ii, **b** ii, **c** ii) and the temporal change centred around the maximum variability (**a** i, **b** i, **c** i) are presented. Coloured lines mark periods of significant increase (red) or decrease (blue). 95% confidence intervals (shaded area) are reported for each predictor (dashed lines).

shell thickness correlated significantly and positively with predation pressure starting in the 1990s[31]. However, it appears unlikely that increased predation pressure also caused the observed shell layer thickening in *N. lapillus* for three reasons. First, *N. lapillus* was absent during the time when predation pressure increased on the Southern North Sea coast, and any thickening related to increased predation pressure would only be reflected in those specimens collected in 2019. Second, we specifically measured shell layer thickness from the dorsal region of the shell and not from the apertural lip to control for predator stress-induced thickening[74] and third, *N. lapillus* specimens also showed a significant increase in aperture size that accompanied the increase in shell thickness (Fig. 7). An increase in aperture size under enhanced predation pressure would be hard to reconcile with the known response of *N. lapillus* to form narrower and smaller apertures and therefore suggests that predation pressure is highly unlikely to be the driver of the observed thickening over the last 130 years. However, our models (Fig. 6) and the observed increase in aperture size (Fig. 7) suggest a significant correlation of shell shape and calcite layer thickness with wind regime trends. Etter (1988)[97] demonstrated that the resistance of *N. lapillus* to increased wave action was proportional to the pedal surface area and thus correlates with larger aperture sizes[74]. This shows that *N. lapillus* exhibits pronounced responses (whether plastic or adaptive is yet to be investigated) to wave exposure and suggests that gradual thickening of the calcite layer could have been a potentially protective response to increased wave action on the Southern North Sea coast as predicted by our models. However, this speculative hypothesis requires a detailed comparative investigation of whole shell thickness responses to varying wave action regimes in this species. Yet, our data provide other more compelling evidence for a general improvement of abiotic and biotic conditions that mitigated global ocean acidification effects and thereby promoted biomineralisation in the study area.

Higher annual temperatures improved calcification conditions. Our models revealed a significant correlation between

temperature and some shell characteristics. Both aragonite layer thickness and aperture size showed significant relationships with mean sea surface temperature (Fig. 6) that increased by 2 °C over the last 130 years along the Southern North Sea coast—inline with global climate change predictions. This increase in mean temperature is a likely candidate to explain the observed shell thickening. For *N. lapillus*, this is not only expected from the kinetics of shell production, as $CaCO_3$ saturation states in sea-water change with temperature but also from a physiological standpoint since metabolic rates and foraging behaviour are temperature-dependent in this species[98–100]. In addition, higher temperatures are also expected to reduce the metabolic energy cost per unit shell due to a proportional reduction of shell organic matter[92,93,96], making higher temperatures generally more favourable for shell formation.

A within-year analysis of the temperature time series from the Southern North Sea coast revealed that winter temperatures (both air and sea surface) increased more rapidly than in the other seasons, indicating increasingly milder winters (Supplementary Fig. 3). Prolonged phases of higher temperatures could have thus allowed for longer periods of biomineralisation during the year (prolonged "calcification windows"), resulting in increased shell layer thickness. This explanation is likely because *N. lapillus* from Whitby on the UK coast did not grow in the laboratory when ambient seawater temperature fell below ~13 °C (i.e., below 13 °C, no noticeable calcification occurred; D.M. personal observation). A similar temperature dependence was also observed by Largen (1967)[98], who reported that there was no growth at temperatures below ~10.5 °C for UK populations and by Hughes (1972)[101], who found that *N. lapillus* populations on the coast of Nova Scotia (Canada) ceased annual growth in October when mean sea surface temperatures usually fall below ~13 °C. An increase in the annual number of days surpassing these growth thresholds, as described by our calcification window estimates, could thus explain the observed increase in shell deposition. In fact, our estimates suggest a relative increase of 58%, or in absolute terms, an increase in 63 days, that reached or surpassed a temperature of
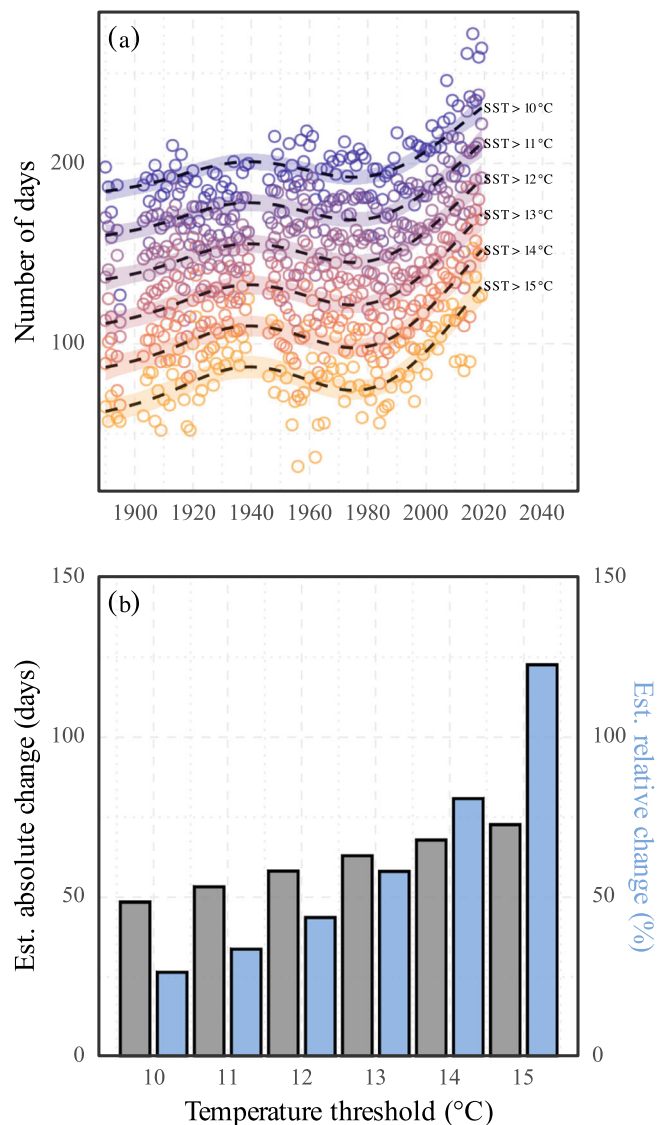
Fig. 4 Estimates of yearly calcification window lengths over the last century. a Historical trends of estimated calcification window length per year expressed as the number of days in which the sea surface temperature exceeds a selected threshold. 95% confidence intervals (shaded area) are reported for each predictor (dashed lines). **b** Absolute and relative change in days exceeding temperature threshold between 1890 and 2019.

13 °C over the last 130 years. Thus, in 2019, *N. lapillus* had 63 more days to calcify (if a calcification threshold of 13 °C applies) than in 1880, which likely resulted in thicker shell layers through secondary thickening (i.e., thickening of the existing shell). However, since secondary shell layer thickening can only occur in the aragonite layer that lines the inside of the shell, prolonged calcification windows would only explain the observed thickening in the aragonite layer but not that in the calcite layer. This is because, in this study, we could only investigate shell thickening but not growth rates in *N. lapillus*. Calcite deposition only occurs at the apertural tip of the shell and variations in calcite thickness are driven by environmental or physiological conditions at the time of growth. This means that the calcite layer measurements are a snapshot of the conditions at the time of primary shell formation. On the contrary, aragonite layer deposition may continue even after primary shell formation which means that if calcification continues over longer intervals it can only result in a thickened aragonite layer.

Nearshore eutrophication mitigated global OA effects. Like ambient temperature, the saturation state of seawater is a crucial variable determining calcification rates. The $CaCO_3$ saturation of seawater is defined as the product of the calcium ion ($[Ca^{2+}]$) and carbonate ion ($[CO_3^{2-}]$) concentrations in the ocean divided by the solubility product (K_{sp}). A reduction in the concentration of either $[Ca^{2+}]$ or $[CO_3^{2-}]$ thus reduces the seawater saturation state, impairing shell formation[102,103] and potentially increases rates of shell dissolution[91]. Lowered seawater salinity is generally associated with lower $[Ca^{2+}]$[104], whereas decreasing seawater pH is accompanied by a shift in solubility that affects the carbonate system resulting in a reduction in $[CO_3^{2-}]$[105].

Median seawater salinity varied significantly between sampling sites in this study by up to 2.6 PSU from 30.1 PSU at Zwarte Polder to 32.7 PSU at Oostende, which is ~85% more than predicted mean salinity changes on the Belgian coast over the last century[31]. This suggests that salinity effects on shell formation in this study, if present, should be stronger on a spatial than a temporal scale. However, when these differences in median salinity are put into perspective in terms of $CaCO_3$ saturation states (Oostende: Ω_{Ca} = 3.8, Ω_{Ar} = 2.4 vs. Zwarte Polder: Ω_{Ca} = 3.7, Ω_{Ar} = 2.3, calculated for seawater with a temperature of 13 °C, pH of 8.1 and total alkalinity of 2300 µmol kg^{-1}) it becomes clear that this small difference in salinity is highly unlikely to have had any effects on shell formation.

In a similar way to the effect of salinity on $[Ca^{2+}]$, the predicted decrease in seawater pH due to global OA is accompanied by a change in the seawater carbonate system, shifting the equilibrium away from the carbonate ion, thereby reducing the $CaCO_3$ saturation state of seawater. Laboratory experiments often find a thinning of shells as a response to OA[3,20], although the opposite has also been reported[15,23]. It appears that species' responses to OA in nature depend on a number of factors and their interactions and may take on unexpected forms, making it difficult to draw general conclusions. For example, a long-term study comparing aragonite percentage in *M. californianus* collected in the 1950s and 2010s reported a significant decrease in aragonite content (as a percentage of whole shell $CaCO_3$) and an increase in calcite content[22]. Although counterintuitive, this finding confirms the observations made by other studies that calcite thickening can be an important response against OA-induced shell dissolution[23,24,31]. Unfortunately, we could not directly assess the effect of pH on shell formation in this study due to a lack of a long-term pH record from the Southern North Sea coast. However, available data from nearshore carbonate system model studies[53,87] show increasing seawater pH for the years 1951 to 1988, followed by overall stable, albeit increasingly more variable, pH conditions[106] in the Dutch and Belgian coastal zone. The increase in pH was attributed to increasing riverine carbon and nutrient loads since the 1960s, causing extensive eutrophication of the Belgian nearshore. This buffered global OA effects and kept mean annual saturation levels high (Ω_{Ar} ~ 2.5 and Ω_{Ca} ~ 4) in the second half of the 20th century[87], providing favourable conditions for *N. lapillus*[107]. In fact, shell shape variability in *N. lapillus* was found to be significantly dependent on the carbonate substrate abundance in a previous study[108]. This means that the observed lack of a shell shape trend (Fig. 2) is in support of a relatively stable carbonate system on the Dutch and Belgian coasts over the studied period and suggests that the observed calcite layer thickening is not a response to OA but is possibly supported by the consistently high $CaCO_3$ substrate abundance. Notably, decreasing trends in seawater pH have been observed in recent years due to regulatory efforts to reduce the level of eutrophication of the Belgian nearshore[106], which will possibly impact the shell formation in future generations of *N. lapillus*.
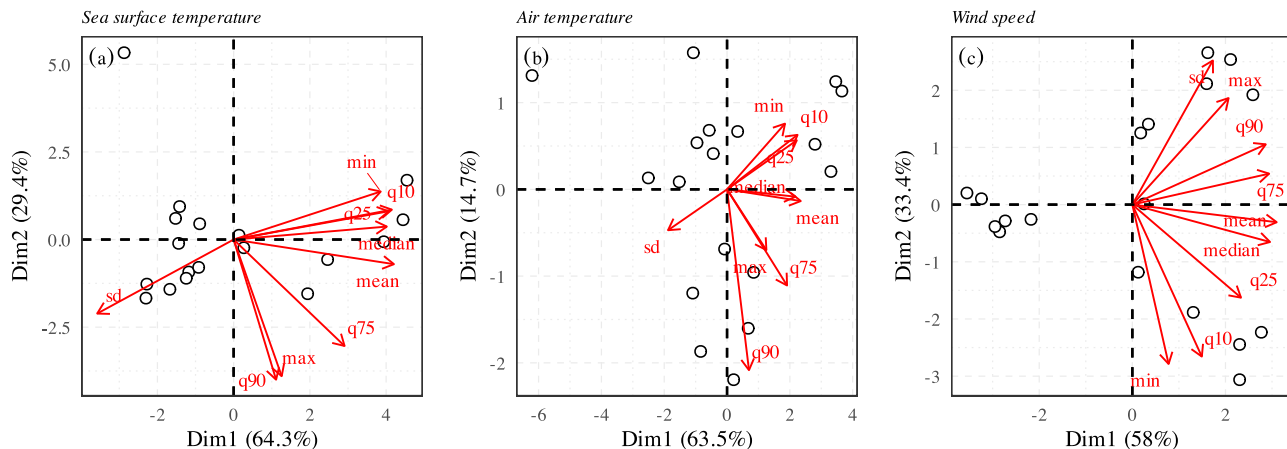
Fig. 5 Biplot of environmental principal component analyses. Biplots of sea surface temperature, air temperature, and wind speed regimes for the Belgian coast from 1890 until 2019 showing the loading of each variable (red arrows) and the PCA scores of each sampling year (points). Arrow directions indicate direction of increasing values of the respective variable and placement of the sampling year indicate how each year is related to the principal components. **a** Biplot of principal component analyses of descriptive statistics for sea surface temperature covering 93.7% of the total variability. **b** PCA biplot of air temperature covering 78.2% of the total variability and **c** PCA biplot of wind speed covering 91.4% of the total variability.
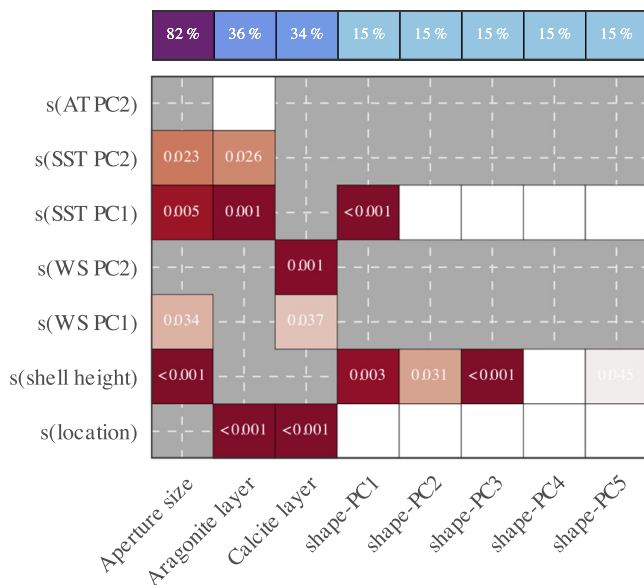

Fig. 6 Correlation matrix of comparative time series analyses. Correlation matrix of comparative model outputs for selected shell characteristics. *y*-axis shows model terms and *x*-axis represents the dependent variables (shell shape and thickness descriptors). Colour intensity (gradient) reflects the significance of correlation given by the models' *p*-values; with darker colours representing lower *p*-values. Included but non-significant model terms ($p > 0.05$) are represented by blanks. The upper bar shows the deviance explained per model in per cent. Colour intensity reflects the amount of deviance explained, with darker colours referring to a higher percentage of deviance explained. The variable s(AT PC1) was not included in any of the models and was thus omitted from the graphic.
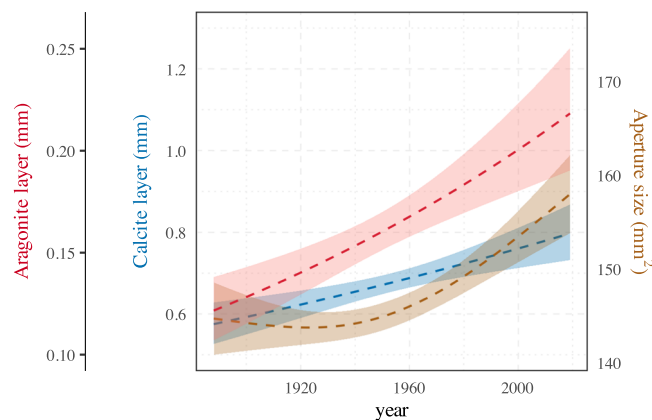

Fig. 7 Generalised Additive Mixed Model shell thickness and aperture trends over the last century. GAMM shell thickness and aperture size trends in the shell of *Nucella lapillus* collected from the Belgian and Dutch coasts between 1888 and 2019. Shaded areas represent the 95% confidence interval.

Possible impact of food abundance. In addition to buffering OA, coastal eutrophication may have had an additional beneficial effect on the carnivorous *N. lapillus* for which there is only anecdotal evidence. Moderate levels of eutrophication can enhance the development of fouling communities[109–111], and high eutrophication levels result in a rapid spreading of the more tolerant species in a community or ecosystem[112–114]. As explained previously, shell formation comes with a cost in metabolic energy, suggesting that food abundance can play a

limiting or supporting role in shell formation[92,93]. Increased eutrophication of the Belgian nearshore reportedly led to more primary production[31,53,106], providing an increasing nutrient supply to filter feeders such as barnacles and blue mussels, both preferred *N. lapillus* prey. In addition, the introduction of the invasive barnacle species *Austrominius modestus* (Darwin, 1854) from New Zealand and southern Australia around 1946[115] and it's rapid spreading on the Southern North Sea coast provided additional food source[116]. Today, *A. modestus* is the dominant barnacle species of the Belgian intertidal fauna[117], densely covering available hard substrata as well as the shells of other organisms (Supplementary Fig. 4; D.M. personal observation). The high abundance of prey in the study area suggests that studied *N. lapillus* populations were provided with sufficient energy to cover the metabolic costs required for shell production during their lifetime, eliminating metabolic energy as a bottleneck during shell formation.

To summarise, observed shell thickening in archival *N. lapillus* from the Belgian and Dutch coasts appears to result from the interaction of multiple abiotic and biotic factors that provided favourable conditions for shell formation throughout the last

130 years. Increasing annual temperatures provided better kinetic and biological conditions for primary shell production and extended annual calcification windows allowed for longer periods of secondary shell layer thickening. In addition, anthropogenically induced eutrophication mitigated global OA effects, maintaining high carbonate saturation states in the study area and further anecdotal evidence points towards a possible influence of enhanced prey abundance on shell formation rates throughout the last century. Our models also suggest a significant effect of wind energy regimes on calcite formation in the shell of *N. lapillus*, but more information is required to substantiate this link. Combined, our long-term shell shape and shell thickness records suggest that studied *N. lapillus* populations appear unaffected by the reported adverse effects of global environmental change. This gives hope that the intertidal rocky-shore community structure on the Southern North Sea may survive predicted future OA scenarios longer than expected, extending the point of no return into the future. Studies like ours demonstrate that museum collections can provide useful ground-truthing data that will serve an important function in future modelling exercises attempting to reconcile large-scale global environmental change impacts on ecosystems[100].

Methods

Sample area and collection. Specimens were collected from seven sites along the Belgian and Dutch coasts (Supplementary Table 1) between 1888 and 2019 and archived at the Royal Belgian Institute of Natural Sciences, Brussels, Belgium (RBINS). Archival specimens were either stored dry or wet in ethanol (70%). All the material used in this study and the preparations are kept at RBINS under loan number R.I.2919.03. The total sampling area extends over ~49 km from the port of Oostende (51°14′N 2°55′E) across the Westerschelde estuary to the beach of Zoutelande (51°29′N 3°28′E) (Supplementary Fig. 2a). The Belgian coast is dominated by wide sandy beaches with little hard substratum, rendering it a generally unsuitable habitat for barnacles, mussels, or the predatory *N. lapillus*. However, the extensive construction of man-made structures against coastal erosion, wave exposure and floodings such as groynes, port structures, and dikes provide excellent substrata for rocky shore organisms and allowed the development of successful populations of these organisms on the Belgian and Dutch coast. In this study, a total of 150 *N. lapillus* specimens were analysed. Only archival specimens with detailed collection dates and location descriptions were included. No samples were available between 1978 and 2019 due to the extensive use of the organotin-compound tributyltin (TBT) as an antifouling agent on ships that caused imposex in female *N. lapillus*[118–120]. The use of TBT led to the local extinction of *N. lapillus* on the Belgian coast in the late 1970s[121], and they only started to reappear in 2012[122]. All specimens collected were adults (likely at sexual maturity) with shell heights > 17 mm[123]. The average shell height of selected specimens was 28.2 ± 2.73 mm (1σ). Shells used here also had intact apices and showed no exterior and interior signs of dissolution or other apparent shell damage.

Environmental dataset. Long-term time series of monthly measurements for wind speed, sea surface temperature and air temperature from 1880 to 2020 in the area of 51°–52°N and 2°–4°E were obtained from the International Comprehensive Ocean–Atmosphere Data Set 3.0[124]. This dataset provides assimilated original marine surface data with traceable data sources and thus provides a reliable data repository with exceptionally high spatial and temporal resolution. Data for sea surface salinity from 1961 to 2018 were obtained from the ICES Dataset on Ocean Hydrography, 2020[125]. Detailed descriptions of all datasets used are provided in the supplementary material.

Due to a lack of robust data, the ICES dataset did not allow for the construction of reliable sea surface salinity time series for every sampling site. However, this was not required as the between site variability in sea surface salinity was expected to be larger than the variability through time[31] and hence an assessment of sampling site salinity variance from available data was more useful. Therefore, we compared salinity values from assimilated data within a 10 km radius around either sampling site. An initial inspection of the data revealed that these were neither normally distributed (Shapiro Wilk test and visual inspection with QQ plots) nor exhibited an equal variance (Levene's test and visual inspections of residuals). Hence, we used a non-parametric Kruskal–Wallis H test and a pairwise Wilcoxon Rank Sum post-hoc test with a standard Bonferroni correction for the comparison of sea surface salinity between sampling sites (Supplementary Table 3).

Shell characteristics. Measurements of shell height, aperture height, and aperture width were made using digital Vernier callipers (± 0.1 mm) for all specimens. Shell shape was evaluated using elliptic Fourier analyses of shell outlines[126,127] following

the approach published elsewhere[108]. For this, individual shells were placed on an illuminated platform with the aperture facing downward in a natural position and images were taken from a fixed distance with a DSLR camera (Nikon 3000 with a Sigma 105 mm macro lens) mounted on a photostand. This produced images of the shells as black silhouettes with sharp edges on a bright background, making them suitable for outline tracing. Outlines were constructed in the position that *N. lapillus* attaches to rocks (i.e., aperture facing downward) rather than in the more commonly used aperture upwards position to study shell shape variations between individuals that are more meaningful to this rocky shore organism, exposed to high wave energy environments. Outlines of individual shells were digitised and turned into $x–y$ coordinates using the R package Momocs[128,129]. Outlines were subsequently smoothed to remove digitisation noise and harmonised regarding orientation and size. Elliptic Fourier analyses were then carried out on the aligned outlines with nine harmonics encompassing 99% of the total harmonic power and a PCA was used to extract axes that reflected most of the shell shape variability among individuals (Supplementary Fig. 1).

The shell layer thickness was analysed by sectioning shells perpendicular to the aperture at the mid-section of the last whorl using a diamond saw (Fig. 1a). The anterior side was embedded in polyester resin (Kleer-Set FF, MetPrep, Coventry, UK). The intersection plane of embedded specimens was smoothed on silicon carbide paper and subsequently polished down to one micron with diamond paste using an automated polishing rig. Micrographs of the shell sections were taken from the dorsal region (Fig. 1a) of the shell halves using a digital stereo microscope (ZEISS Primo Star, Zeiss, Oberkochen, Germany). Since aperture thickness is influenced by both predation pressure and wave exposure in *N. lapillus* through the formation of thicker apertural lips and/or teeth[58–60,65], measurements of shell layer thickness further inside the shell provide a better proxy for environmentally induced shell layer thickness variability. Aragonite and calcite layer thicknesses were individually measured from 10 randomly chosen regions within the micrographs using the software ZEISS Labscope (v.3.1). For this purpose, 10 approximately equally distanced sections were selected on either micrograph, and total shell thickness and calcite layer thickness were measured perpendicular to the innermost aragonite layer of the shells. Aragonite layer thickness was inferred by subtracting calcite layer thickness from total shell thickness. To validate the reproducibility of this method, the same images were evaluated three times in different orders and on different days showing no statistically significant difference between measurement sessions (Kruskal–Wallis H test, $H(2) = 1.029$, $p = 0.598$). Mean shell layer thicknesses were then calculated from all 30 measurements per shell of each individual sample (Fig. 1).

Environmental time series analysis. Long-term time series (1880–2020) of sea surface temperature, air temperature and wind speed were modelled with GAMMs using the R package mgcv[130] and following protocols for data exploration and regression-type analyses[131,132]. Each environmental variable was modelled using month and year as fixed covariates and their tensor product interaction term. Years were included using thin plate regression splines, and months were included using cubic regression splines with the number of knots limited to 12. Plots of the partial autocorrelation function showed significant autocorrelation of the residuals which required the use of autoregressive models to account for the temporal autocorrelation. To identify significant trend changes in the modelled time series, the first derivative of the fitted model was calculated using finite differences. Since the equation of the regression splines is unknown, finite differences provide a method to resample a fitted spline with a chosen number of points. This enabled us to calculate the first derivative of a fitted regression line through these resampled points, which resembles a close approximation of the fitted spline.

Yearly calcification windows were constructed from monthly mean temperatures and their standard deviations. This was done by estimating the percentage of a given month above either temperature threshold using monthly mean and standard deviation temperature data (assuming that temperatures were normally distributed) and converting percentages into days for every given month. Temperature threshold regression trends were then formulated using GAMs, including year, the number of available observations per year, and calcification thresholds (10–15 °C) as predictors.

Shell characteristics time series analysis. Correlations of selected shell shape and thickness trends, namely aperture size, shape-PC1–shape-PC5, calcite layer thickness and aragonite layer thickness, with sampling year, shell height and sampling site were examined by GAMMs. Given that shape-PC1–shape-PC5 were shape representatives of the same shell, normalised shape descriptors were modelled simultaneously within the same GAMM to allow for a holistic shape description[71]. All GAMMs included sampling year as a continuous variable to examine long-term trends among shell descriptors and shell height as a continuous variable to account for morphological and compositional biases due to allometric scaling. Sampling site was included as a random-effect term to account for dependencies among observations from the same sampling site in all models. An initial data exploration using variograms showed no significant spatial autocorrelation in the data, and therefore, no spatial autocorrelation structures were deemed necessary. Inspections using (partial) autocorrelation plots of model residuals also showed no temporal autocorrelation.

Comparative time series analysis. The effect of long-term environmental change in wind speed, sea surface temperature, and air temperature on selected shell descriptors was analysed by a sequence of comparative models. Therefore, descriptive statistics for each environmental variable were calculated (i.e., mean, median, min, max, 10th percentile, 25th percentile, 75th percentile, 90th percentile, and standard deviation). To account for the natural variability spectrum that individual specimens experienced throughout their lifetime, the descriptive statistics were calculated for a time window encompassing three years up to the sampling year of the respective samples. A PCA was then performed on the normalised descriptive statistics for each environmental parameter to describe temperature and wind speed "regimes" (Fig. 3)[6,31]. This helped to reduce dimensionality in the data and allowed us to model more complex relationships while avoiding multi-collinearity issues among explanatory variables. GAMMs were then constructed for each of the selected shell characteristics including the first two principal components of each environmental regime as independent variables. An automated variable selection process using the dredge function in the R package *MuMIn* v.1.43.17[133] was used to assess model fits for all possible combinations of covariates and the best acceptable model (identified by the Akaike's information criterion[134]) with a CORVIF factor < 3 was selected. In all global models, the smoothing parameter was limited ($k = 3$) to only allow monotonic relationships. As with the shell characteristics GAMMs described in the previous section, models describing shell shapes also included all shape-PCs simultaneously within the same model for an integrated description of shape relationships. The sampling site was included in all models as a random-effect term.

Reporting summary. Further information on research design is available in the Nature Research Reporting Summary linked to this article.

Data availability

Datasets generated during this study are made publicly available on the following Github repository: dm807cam/nucella2021belgium.

Code availability

All R scripts produced for this study are made publicly available on the following Github repository: dm807cam/nucella2021belgium.

References

1. Byrne, M. Impact of ocean warming and ocean acidification on marine invertebrate life history stages: vulnerabilities and potential for persistence in a changing ocean. *Oceanogr. Mar. Biol. Annu. Rev.* **49**, 1–42 (2011).
2. Byrne, M. & Przeslawski, R. Multistressor impacts of warming and acidification of the ocean on marine invertebrates' life histories. *Integr. Comp. Biol.* **53**, 582–596 (2013).
3. Fitzer, S. C. et al. Ocean acidification and temperature increase impact mussel shell shape and thickness: problematic for protection? *Ecol. Evol.* **5**, 4875–4884 (2015).
4. Hofmann, G. E. et al. The effect of ocean acidification on calcifying organisms in marine ecosystems: an Organism-to-Ecosystem perspective. *Annu. Rev. Ecol. Evol. Syst.* **41**, 127–147 (2010).
5. Kroeker, K. J. et al. Impacts of ocean acidification on marine organisms: quantifying sensitivities and interaction with warming. *Glob. Chang. Biol.* **19**, 1884–1896 (2013).
6. Kroeker, K. J. et al. Interacting environmental mosaics drive geographic variation in mussel performance and predation vulnerability. *Ecol. Lett.* **19**, 771–779 (2016).
7. Parker, L. M. et al. Predicting the response of molluscs to the impact of ocean acidification. *Biology* **2**, 651–692 (2013).
8. Przeslawski, R., Byrne, M. & Mellin, C. A review and meta-analysis of the effects of multiple abiotic stressors on marine embryos and larvae. *Glob. Chang. Biol.* **21**, 2122–2140 (2015).
9. Suckling, C. C. et al. Adult acclimation to combined temperature and pH stressors significantly enhances reproductive outcomes compared to short-term exposures. *J. Anim. Ecol.* **84**, 773–784 (2015).
10. Thomsen, J., Haynert, K., Wegner, K. M. & Melzner, F. Impact of seawater carbonate chemistry on the calcification of marine bivalves. *Biogeosciences* **12**, 4209–4220 (2015).
11. Waldbusser, G. G. et al. Saturation-state sensitivity of marine bivalve larvae to ocean acidification. *Nat. Clim. Chang.* **5**, 273–280 (2014).
12. Waldbusser, G. G. et al. Ocean acidification has multiple modes of action on bivalve larvae. *PLoS ONE* **10**, e0128376 (2015).
13. Barclay, K. M. et al. Variation in the effects of ocean acidification on shell growth and strength in two intertidal gastropods. *Mar. Ecol. Prog. Ser.* **626**, 109–121 (2019).
14. Byrne, M. & Fitzer, S. The impact of environmental acidification on the microstructure and mechanical integrity of marine invertebrate skeletons. *Conserv. Physiol.* **7**, coz062 (2019).
15. Cross, E. L., Peck, L. S. & Harper, E. M. Ocean acidification does not impact shell growth or repair of the Antarctic brachiopod *Liothyrella uva* (Broderip, 1833). *J. Exp. Mar. Biol. Ecol.* **462**, 29–35 (2015).
16. Cross, E. L., Peck, L. S., Lamare, M. D. & Harper, E. M. No ocean acidification effects on shell growth and repair in the New Zealand brachiopod *Calloria inconspicua* (Sowerby, 1846). *ICES J. Mar. Sci.* **73**, 920–926 (2015).
17. Doney, S. C., Fabry, V. J., Feely, R. A. & Kleypas, J. A. Ocean acidification: The other CO_2 problem. *Annu. Rev. Mar. Sci.* **1**, 169–192 (2009).
18. Watson, S.-A. et al. Marine invertebrate skeleton size varies with latitude, temperature and carbonate saturation: implications for global change and ocean acidification. *Glob. Chang. Biol.* **18**, 3026–3038 (2012).
19. Fitzer, S. C., Cusack, M., Phoenix, V. R. & Kamenos, N. A. Ocean acidification reduces the crystallographic control in juvenile mussel shells. *J. Struct. Biol.* **188**, 39–45 (2014).
20. Gaylord, B. et al. Functional impacts of ocean acidification in an ecologically critical foundation species. *J. Exp. Biol.* **214**, 2586–2594 (2011).
21. Gazeau, F. et al. Impacts of ocean acidification on marine shelled molluscs. *Mar. Biol.* **160**, 2207–2245 (2013).
22. Bullard, E. M., Torres, I., Ren, T., Graeve, O. A. & Roy, K. Shell mineralogy of a foundational marine species, *Mytilus californianus*, over half a century in a changing ocean. *Proc. Natl. Acad. Sci. USA* **118**, e2004769118 (2021).
23. Cross, E. L., Harper, E. M. & Peck, L. S. Thicker shells compensate extensive dissolution in brachiopods under future ocean acidification. *Environ. Sci. Technol.* **53**, 5016–5026 (2019).
24. Harper, E. M. Are calcitic layers an effective adaptation against shell dissolution in the Bivalvia? *J. Zool.* **251**, 179–186 (2000).
25. Ashton, G. V., Morley, S. A., Barnes, D. K. A., Clark, M. S. & Peck, L. S. Warming by 1 °C drives species and assemblage level responses in Antarctica's marine shallows. *Curr. Biol.* **27**, 2698–2705.e3 (2017).
26. Cornwall, C. E. et al. A coralline alga gains tolerance to ocean acidification over multiple generations of exposure. *Nat. Clim. Chang.* **10**, 143–146 (2020).
27. Donelson, J. M., Salinas, S., Munday, P. L. & Shama, L. N. S. Transgenerational plasticity and climate change experiments: where do we go from here? *Glob. Chang. Biol.* **24**, 13–34 (2018).
28. Gibbin, E. M., Massamba N'Siala, G., Chakravarti, L. J., Jarrold, M. D. & Calosi, P. The evolution of phenotypic plasticity under global change. *Sci. Rep.* **7**, 17253 (2017).
29. Peck, L. S. Organisms and responses to environmental change. *Mar. Genom.* **4**, 237–243 (2011).
30. Somero, G. N. The physiology of global change: linking patterns to mechanisms. *Annu. Rev. Mar. Sci.* **4**, 39–61 (2012).
31. Telesca, L., Peck, L. S., Backeljau, T., Heinig, M. F. & Harper, E. M. A century of coping with environmental and ecological changes via compensatory biomineralization in mussels. *Glob. Chang. Biol.* **27**, 624–639 (2021).
32. Kroeker, K. J. et al. Ecological change in dynamic environments: accounting for temporal environmental variability in studies of ocean change biology. *Glob. Chang. Biol.* **26**, 54–67 (2020).
33. Bernhardt, J. R., Sunday, J. M., Thompson, P. L. & O'Connor, M. I. Nonlinear averaging of thermal experience predicts population growth rates in a thermally variable environment. *Proc. Biol. Sci.* **285**, 20181076 (2018).
34. Harley, C. D. G. et al. Conceptualizing ecosystem tipping points within a physiological framework. *Ecol. Evol.* **7**, 6035–6045 (2017).
35. Griffiths, J. S., Pan, T.-C. F. & Kelly, M. W. Differential responses to ocean acidification between populations of *Balanophyllia elegans* corals from high and low upwelling environments. *Mol. Ecol.* **28**, 2715–2730 (2019).
36. Telesca, L. et al. Biomineralization plasticity and environmental heterogeneity predict geographical resilience patterns of foundation species to future change. *Glob. Chang. Biol.* **25**, 4179–4193 (2019).
37. Barnes, D. K. A., Ashton, G. V., Morley, S. A. & Peck, L. S. 1 °C warming increases spatial competition frequency and complexity in antarctic marine macrofauna. *Commun. Biol.* **4**, 208 (2021).
38. Cross, E. L., Harper, E. M. & Peck, L. S. A 120-year record of resilience to environmental change in brachiopods. *Glob. Chang. Biol.* **24**, 2262–2271 (2018).
39. Kidwell, S. M. Biology in the anthropocene: challenges and insights from young fossil records. *Proc. Natl Acad. Sci. USA* **112**, 4922–4929 (2015).
40. Pfister, C. A. et al. Historical baselines and the future of shell calcification for a foundation species in a changing ocean. *Proc. Biol. Sci.* **283**, 20160392 (2016).
41. Angilletta, M. J., Jr Zelic, M. H., Adrian, G. J., Hurliman, A. M. & Smith, C. D. Heat tolerance during embryonic development has not diverged among

populations of a widespread species (*Sceloporus undulatus*). *Conserv. Physiol.* **1**, cot018 (2013).

42. Hofmann, G. E. & Somero, G. Evidence for protein damage at environmental temperatures: Seasonal changes in levels of ubiquitin conjugates and hsp70 in the intertidal mussel *Mytilus trossulus*. *J. Exp. Biol.* **198**, 1509–1518 (1995).

43. Roberts, D. A., Hofmann, G. E. & Somero, G. N. Heat-Shock protein expression in *Mytilus californianus*: Acclimatization (seasonal and Tidal-Height comparisons) and acclimation effects. *Biol. Bull.* **192**, 309–320 (1997).

44. Easterling, D. R. et al. Climate extremes: observations, modeling, and impacts. *Science* **289**, 2068–2074 (2000).

45. Meehl, G. A. & Tebaldi, C. More intense, more frequent, and longer lasting heat waves in the 21st century. *Science* **305**, 994–997 (2004).

46. Rahmstorf, S. & Coumou, D. Increase of extreme events in a warming world. *Proc. Natl Acad. Sci. USA* **108**, 17905–17909 (2011).

47. Rummukainen, M. Changes in climate and weather extremes in the 21st century. *Wiley Interdiscip. Rev. Clim. Change* **3**, 115–129 (2012).

48. Nehls, G. & Thiel, M. Large-scale distribution patterns of the mussel *Mytilus edulis* in the Wadden Sea of Schleswig-Holstein: do storms structure the ecosystem? *Neth. J. Sea Res.* **31**, 181–187 (1993).

49. Sorte, C. J. B. et al. Thermal tolerance limits as indicators of current and future intertidal zonation patterns in a diverse mussel guild. *Mar. Biol.* **166**, https://doi.org/10.1007/s00227-018-3452-6 (2019).

50. Gao, Y. et al. Evolution of trace metal and organic pollutant concentrations in the Scheldt River Basin and the Belgian Coastal Zone over the last three decades. *J. Mar. Syst.* **128**, 52–61 (2013).

51. Camphuysen, K. & Vollaard, B. Oil pollution in the Dutch sector of the North Sea. In *Oil Pollution in the North Sea* (ed., Carpenter, A.) 117–140 (Springer International Publishing, 2016).

52. Brion, N., Jans, S., Chou, L. & Rousseau, V. Nutrient loads to the Belgian coastal zone. In *Current Status of Eutrophication in the Belgian Coastal Zone* (eds Rousseau, V., Lancelot, C. & Cox, D.) 17–43 (Presses Universitaires de Bruxelles, Brussels, 2008).

53. Gypens, N., Borges, A. V. & Lancelot, C. Effect of eutrophication on air-sea CO_2 fluxes in the coastal Southern North Sea: a model study of the past 50 years. *Glob. Chang. Biol.* **15**, 1040–1056 (2009).

54. Mackenzie, F. T., Ver, L. M. & Lerman, A. Century-scale nitrogen and phosphorus controls of the carbon cycle. *Chem. Geol.* **190**, 13–32 (2002).

55. Burrows, M. T. & Hughes, R. N. Natural foraging of the dogwhelk, *Nucella lapillus* (Linnaeus); the weather and whether to feed. *J. Moll. Stud.* **55**, 285–295 (1989).

56. Hughes, R. N. & Burrows, M. T. An interdisciplinary approach to the study of foraging behaviour in the predatory gastropod, *Nucella lapillus* (L.). *Ethol. Ecol. Evol.* **6**, 75–85 (1994).

57. Trussell, G. C., Ewanchuk, P. J. & Bertness, M. D. Trait-mediated effects in rocky intertidal food chains: predator risk cues alter prey feeding rates. *Ecology* **84**, 629–640 (2003).

58. Palmer, A. R. Effect of crab effluent and scent of damaged conspecifics on feeding, growth, and shell morphology of the Atlantic dogwhelk *Nucella lapillus* (L.). *Hydrobiologia* **193**, 155–182 (1990).

59. Pascoal, S., Carvalho, G., Creer, S., Mendo, S. & Hughes, R. N. Plastic and heritable variation in shell thickness of the intertidal gastropod *Nucella lapillus* associated with risks of crab predation and wave action, and sexual maturation. *PLoS ONE* **7**, e52134 (2012).

60. Avery, R. & Etter, R. J. Microstructural differences in the reinforcement of a gastropod shell against predation. *Mar. Ecol. Prog. Ser.* **323**, 159–170 (2006).

61. Mayk, D. Transitional spherulitic layer in the muricid *Nucella lapillus*. *J. Molluscan Stud.* **87**, https://doi.org/10.1093/mollus/eyaa035 (2020).

62. Berry, R. J. & Crothers, J. H. Visible variation in the dog whelk, *Nucella lapillus*. *J. Zool.* **174**, 123–148 (1974).

63. Crothers, J. H. Two different patterns of shell-shape variation in the dog-whelk *Nucella lapillus* (L.). *Biol. J. Linn. Soc. Lond.* **25**, 339–353 (1985).

64. Galante-Oliveira, S., Marçal, R., Pacheco, M. & Barroso, C. M. *Nucella lapillus* ecotypes at the southern distributional limit in Europe: Variation in shell morphology is not correlated with chromosome counts on the Portuguese Atlantic coast. *J. Mollusc. Stud.* **78**, 147–150 (2011).

65. Appleton, R. D. & Palmer, A. R. Water-borne stimuli released by predatory crabs and damaged prey induce more predator-resistant shells in a marine gastropod. *Proc. Natl Acad. Sci. USA* **85**, 4387–4391 (1988).

66. Cowell, E. B. & Crothers, J. H. On the occurrence of multiple rows of 'teeth' in the shell of the dog-whelk *Nucella lapillus*. *J. Mar. Biol. Assoc. UK* **50**, 1101–1111 (1970).

67. Currey, J. D. & Hughes, R. N. Strength of the dogwhelk *Nucella lapillus* and the winkle *Littorina littorea* from different habitats. *J. Anim. Ecol.* **51**, 47–56 (1982).

68. Hughes, R. N. & Elner, R. W. Tactics of a predator, *Carcinus maenas*, and morphological responses of the prey, *Nucella lapillus*. *J. Anim. Ecol.* **48**, 65–78 (1979).

69. Vermeij, G. J. & Currey, J. D. Geographical variation in the shell strength of thaidid snail shells. *Biol. Bull.* **158**, 383–389 (1980).

70. Benedetti-Cecchi, L. & Trussell, G. C. Rocky intertidal communities. In *Marine Community Ecology and Conservation* 203–225 (Sinauer Associates, Sunderland, MA, 2014).

71. Telesca, L. et al. Blue mussel shell shape plasticity and natural environments: a quantitative approach. *Sci. Rep.* **8**, 2865 (2018).

72. Cooke, A. H. & Reed, F. R. C. *The Cambridge Natural History* (Macmillan Company, 1895).

73. Kitching, J. A. & Ebling, F. J. In *Ecological Studies at Lough Ine* Vol. 4 197–291 (ed. Cragg, J. B.) (Academic Press, 1967).

74. Crothers, J. H. Dog-whelks: an introduction to the biology of *Nucella lapillus* (L.). *Field Stud.* **6**, 291–360 (1985).

75. Chadwick, M., Harper, E. M., Lemasson, A., Spicer, J. I. & Peck, L. S. Quantifying susceptibility of marine invertebrate biocomposites to dissolution in reduced pH. *R. Soc. Open Sci.* **6**, 190252 (2019).

76. Laing, I. Effect of temperature and ration on growth and condition of king scallop (*Pecten maximus*) spat. *Aquaculture* **183**, 325–334 (2000).

77. Thouzeau, G. et al. Growth of *Argopecten purpuratus* (Mollusca: Bivalvia) on a natural bank in Northern Chile: sclerochronological record and environmental controls. *Aquat. Living Resour.* **21**, 45–55 (2008).

78. Kleinman, S., Hatcher, B. G., Scheibling, R. E., Taylor, L. H. & Hennigar, A. W. Shell and tissue growth of juvenile sea scallops (*Placopecten magellanicus*) in suspended and bottom culture in Lunenburg Bay, Nova Scotia. *Aquaculture* **142**, 75–97 (1996).

79. Doroudi, M. S., Southgate, P. C. & Mayer, R. J. The combined effects of temperature and salinity on embryos and larvae of the black lip pearl oyster, *Pinctada margaritifera* (L.). *Aquacult. Res.* **30**, 271–277 (1999).

80. Tomaru, Y., Kumatabara, Y., Kawabata, Z. & Nakano, S. Effect of water temperature and chlorophyll abundance on shell growth of the Japanese pearl oyster, *Pinctada fucata martensii*, in suspended culture at different depths and sites. *Aquacult. Res.* **33**, 109–116 (2002).

81. Schöne, B., Tanabe, K., Dettman, D. & Sato, S. Environmental controls on shell growth rates and $\delta^{18}O$ of the shallow-marine bivalve mollusk *Phacosoma japonicum* in Japan. *Mar. Biol.* **142**, 473–485 (2003).

82. Ballesta-Artero, I., Witbaard, R., Carroll, M. L. & Meer, J van der Environmental factors regulating gaping activity of the bivalve *Arctica islandica* in northern Norway. *Mar. Biol.* **164**, 116 (2017).

83. Witbaard, R. Growth variations in *Arctica islandica* L. (Mollusca): a reflection of hydrography-related food supply. *ICES J. Mar. Sci.* **53**, 981–987 (1996).

84. Joubert, C. et al. Temperature and food influence shell growth and mantle gene expression of shell matrix proteins in the pearl oyster *Pinctada margaritifera*. *PLoS ONE* **9**, e103944 (2014).

85. Fay, A. R. & McKinley, G. A. Global trends in surface ocean pCO_2 from in situ data. *Global Biogeochem. Cycles* **27**, 541–557 (2013).

86. Ostle, C. et al. *Carbon Dioxide and Ocean Acidification Observations in UK Waters*. Synthesis report with a focus on 2010–2015. 44 https://doi.org/10.13140/RG.2.1.4819.4164 (2016).

87. Borges, A. V. & Gypens, N. Carbonate chemistry in the coastal zone responds more strongly to eutrophication than ocean acidification. *Limnol. Oceanogr.* **55**, 346–353 (2010).

88. Clarke, A. & Beaumont, J. C. An extreme marine environment: a 14-month record of temperature in a polar tidepool. *Polar Biol.* **43**, 2021–2030 (2020).

89. Fisher, J. A. D., Rhile, E. C., Liu, H. & Petraitis, P. S. An intertidal snail shows a dramatic size increase over the past century. *Proc. Natl Acad. Sci. USA* **106**, 5209–5212 (2009).

90. Clarke, A. Seasonal acclimatization and latitudinal compensation in metabolism: Do they exist? *Funct. Ecol.* **7**, 139–149 (1993).

91. Sanders, T., Thomsen, J., Müller, J. D., Rehder, G. & Melzner, F. Decoupling salinity and carbonate chemistry: low calcium ion concentration rather than salinity limits calcification in Baltic Sea mussels. *Biogeosciences* **18**, 2573–2590 (2021).

92. Palmer, A. R. Relative cost of producing skeletal organic matrix versus calcification: evidence from marine gastropods. *Mar. Biol.* **75**, 287–292 (1983).

93. Palmer, A. R. Calcification in marine molluscs: how costly is it? *Proc. Natl. Acad. Sci. USA* **89**, 1379–1382 (1992).

94. Watson, S.-A., Morley, S. A. & Peck, L. S. Latitudinal trends in shell production cost from the tropics to the poles. *Sci. Adv.* **3**, e1701362 (2017).

95. Burton, E. A. & Walter, L. M. Relative precipitation rates of aragonite and Mg calcite from seawater: temperature or carbonate ion control? *Geology* **15**, 111–114 (1987).

96. Sanders, T., Schmittmann, L., Nascimento-Schulze, J. C. & Melzner, F. High calcification costs limit mussel growth at low salinity. *Front. Mar. Sci.* **5**, 352 (2018).

97. Etter, R. J. Assymmetrical development plasticity in an intertidal snail. *Evolution* **42**, 322–334 (1988).

98. Largen, M. J. The influence of water temperature upon the life of the dog-whelk *Thais lapillus* (Gastropoda: Prosobranchia). *J. Anim. Ecol.* **36**, 207–214 (1967).

99. Stickle, W. B., Moore, M. N. & Bayne, B. L. Effects of temperature, salinity and aerial exposure on predation and lysosomal stability of the dogwhelk *Thais* (*Nucella*) *lapillus* (L.). *J. Exp. Mar. Biol. Ecol.* **93**, 235–258 (1985).

100. Queirós, A. M. et al. Scaling up experimental ocean acidification and warming research: from individuals to the ecosystem. *Glob. Chang. Biol.* **21**, 130–143 (2015).

101. Hughes, R. N. Annual production of two Nova Scotian populations of *Nucella lapillus* (L.). *Oecologia* **8**, 356–370 (1972).

102. Gattuso, J.-P., Frankignoulle, M., Bourge, I., Romaine, S. & Buddemeier, R. W. Effect of calcium carbonate saturation of seawater on coral calcification. *Glob. Planet. Change* **18**, 37–46 (1998).

103. Schneider, K. & Erez, J. The effect of carbonate chemistry on calcification and photosynthesis in the hermatypic coral *Acropora eurystoma*. *Limnol. Oceanogr.* **51**, 1284–1293 (2006).

104. Kremling, K. & Wilhelm, G. Recent increase of the calcium concentrations in baltic sea waters. *Mar. Pollut. Bull.* **34**, 763–767 (1997).

105. Riebesell, U., Fabry, V. J., Hansson, L. & Gattuso, J.-P. *Guide to Best Practices for Ocean Acidification Research and Data Reporting* (Office for Official Publications of the European Communities, 2011).

106. Desmit, X. et al. Changes in chlorophyll concentration and phenology in the North Sea in relation to de eutrophication and sea surface warming. *Limnol. Oceanogr.* **65**, 828–847 (2020).

107. Petraitis, P. S. & Dudgeon, S. R. Declines over the last two decades of five intertidal invertebrate species in the western North Atlantic. *Commun. Biol.* **3**, 591 (2020).

108. Mayk, D., Peck, L. S. & Harper, E. M. Evidence for carbonate system mediated shape shift in an intertidal predatory gastropod. *Front. Mar. Sci.* **9**, 894182 (2022).

109. Page, H. M. & Hubbard, D. M. Temporal and spatial patterns of growth in mussels *Mytilus edulis* on an offshore platform: relationships to water temperature and food availability. *J. Exp. Mar. Biol. Ecol.* **111**, 159–179 (1987).

110. Thomsen, J., Casties, I., Pansch, C., Körtzinger, A. & Melzner, F. Food availability outweighs ocean acidification effects in juvenile *Mytilus edulis*: laboratory and field experiments. *Glob. Chang. Biol.* **19**, 1017–1027 (2013).

111. Wołowicz, M., Sokołowski, A., Bawazir, A. S. & Lasota, R. Effect of eutrophication on the distribution and ecophysiology of the mussel *Mytilus trossulus* (Bivalvia) in southern Baltic Sea (the Gulf of Gdańsk). *Limnol. Oceanogr.* **51**, 580–590 (2006).

112. Moran, P. J & Grant, T. R. The effects of industrial pollution on the development and succession of marine fouling communities I. Analysis of species richness and frequency data. *Mar. Ecol.* **10**, 231–246 (1989).

113. Moran, P. J. & Grant, T. R. Transference of marine fouling communities between polluted and unpolluted sites: impact on structure. *Environ. Pollut.* **72**, 89–102 (1991).

114. Rastetter, E. B. & Cooke, W. J. Responses of marine fouling communities to sewage abatement in Kaneohe Bay, Oahu, Hawaii. *Mar. Biol.* **53**, 271–280 (1979).

115. Boschma, H. *Elminius modestus* in the Netherlands. *Nature* **161**, 403–404 (1948).

116. Wolff, W. J. Non-indigenous marine and estuarine species in the Netherlands. *Zool. Meded.* **79-1**, 1–116 (2005).

117. Kerckhof, F. Barnacles (Cirripedia, Balanomorpha) in Belgian waters, an overview of the species and recent evolutions, with emphasis on exotic species. *Bull. Inst. R. Sci. Nat. Belg. Biol./Bull. K. Belg. Inst. Natuurwet. Biol.* **72**, 93–104 (2002).

118. Gibbs, P. E., Bryan, G. W. & Pascoe, P. L. TBT-induced imposex in the dogwhelk, *Nucella lapillus*: geographical uniformity of the response and effects. *Mar. Environ. Res.* **32**, 79–87 (1991).

119. Gibbs, P. E. *Biological Effects of Contaminants: Use of Imposex in the Dogwhelk (Nucella lapillus) as a Bioindicator of Tributyltin Pollution.* 37 https://doi.org/10.25607/OBP-272 (1999).

120. Oehlmann, J. et al. Imposex in *Nucella lapillus* and intersex in *Littorina littorea*: Interspecific comparison of two TBT-induced effects and their geographical uniformity. In *Aspects of Littorinid Biology* (eds O'Riordan, R. M., Burnell, G. M., Davies, M. S. & Ramsay, N. F.) 199–213 (Springer Netherlands, 1998).

121. Kerckhof, F. Over het verdwijnen van de purperslak *Nucella lapillus* (Linnaeus, 1758), langs onze kust. *De Strandvlo* **8**, 82–85 (1988).

122. De Blauwe, H. & D'Udekem d'Acoz, C. Voortplantende populatie van de purperslak (*Nucella lapillus*) in België na meer dan 30 jaar afwezigheid (Mollusca, Gastropoda, Muricidae). *De Strandvlo* **32**, 127–131 (2012).

123. Galante-Oliveira, S. et al. Factors affecting RPSI in imposex monitoring studies using *Nucella lapillus* (L.) as bioindicator. *J. Environ. Monit.* **12**, 1055–1063 (2010).

124. National Centers for Environmental Information/NESDIS/NOAA/U.S. Department of Commerce et al. *International Comprehensive*

Ocean–Atmosphere Data Set (ICOADS) Release 3, Monthly Summaries https://doi.org/10.5065/D6V40SFD (2016).

125. ICES. *Dataset on Ocean Hydrography* (ICES, 2020).

126. Giardina, C. R. & Kuhl, F. P. Accuracy of curve approximation by harmonically related vectors with elliptical loci. *Comput. Graph. Image Process.* **6**, 277–285 (1977).

127. Kuhl, F. P. & Giardina, C. R. Elliptic fourier features of a closed contour. *Comput. Graph. Image Process.* **18**, 236–258 (1982).

128. Bonhomme, V., Picq, S., Gaucherel, C. & Claude, J. Momocs: outline analysis using R. *J. Stat. Softw.* **56**, 1–24 (2014).

129. R Core Team. *R: A Language and Environment for Statistical Computing* (R Core Team, 2020).

130. Wood, S. N. Fast stable restricted maximum likelihood and marginal likelihood estimation of semiparametric generalized linear models. *J. R. Stat. Soc. Ser. B Stat. Methodol.* **73**, 3–36 (2011).

131. Zuur, A. F., Ieno, E. N. & Elphick, C. S. A protocol for data exploration to avoid common statistical problems. *Methods Ecol. Evol.* **1**, 3–14 (2010).

132. Zuur, A. F. & Ieno, E. N. A protocol for conducting and presenting results of regression-type analyses. *Methods Ecol. Evol.* **7**, 636–645 (2016).

133. Bartoń, K. MuMIn: Multi-Model Inference https://cran.r-project.org/web/packages/MuMIn/index.html (2020).

134. Akaike, H. Information theory and an extension of the maximum likelihood principle. *Springer Ser. Stat.* 610–624 https://doi.org/10.1007/978-1-4612-0919-5/_38 (1992).

Acknowledgements

Author contributions

D.M., L.S.P., T.B. and E.M.H. conceived the original project; D.M. sampled the museum collections, performed the laboratory work, data assimilation, and modelling work; T.B. provided the archival specimens and collected the living specimens; D.M. wrote the first draft of the manuscript, and all co-authors contributed substantially to revisions.

Competing interests

The authors declare no competing interests.

Additional information

Supplementary information The online version contains supplementary material available at https://doi.org/10.1038/s43247-022-00486-7.

Correspondence and requests for materials should be addressed to Dennis Mayk.

Peer review information *Communications Earth & Environment* thanks Niels de Winter and the other, anonymous, reviewer(s) for their contribution to the peer review of this work. Primary Handling Editors: Ola Kwiecien and Clare Davis.

Reprints and permission information is available at http://www.nature.com/reprints

Publisher's note Springer Nature remains neutral with regard to jurisdictional claims in published maps and institutional affiliations.